Hindawi Publishing Corporation
Advances in Condensed Matter Physics
Volume 2013, Article ID 382140, 5 pages
http://dx.doi.org/10.1155/2013/382140

Research Article

Temperature Dependence of Electrical Properties and Crystal Structure of $0.29Pb(In_{1/2}Nb_{1/2})O_3$–$0.44Pb(Mg_{1/3}Nb_{2/3})O_3$–$0.27PbTiO_3$ Single Crystals

Qian Li,[1] Yun Liu,[1] Andrew Studer,[2] Zhenrong Li,[3] Ray Withers,[1] and Zhuo Xu[3]

[1] *Research School of Chemistry, The Australian National University, ACT 0200, Australia*
[2] *Bragg Institute, Australian Nuclear Science and Technology Organization (ANSTO), NSW 2232, Australia*
[3] *Electronic Materials Research Laboratory, Xi'an Jiaotong University, Shanxi 7100049, China*

Correspondence should be addressed to Yun Liu; yliu@rsc.anu.edu.au

Received 31 May 2013; Revised 3 October 2013; Accepted 7 October 2013

Academic Editor: Jianhua Hao

We characterized the temperature dependent (~25–200°C) electromechanical properties and crystal structure of $Pb(In_{1/2}Nb_{1/2})O_3$-$Pb(Mg_{1/3}Nb_{2/3})O_3$-$PbTiO_3$ single crystals using *in situ* electrical measurement and neutron diffraction techniques. The results show that the poled crystal experiences an addition phase transition around 120°C whereas such a transition is absent in the unpoled crystal. It is also found that the polar order persists above the maximum dielectric permittivity temperature at which the crystal shows a well-defined antiferroelectric behavior. The changes in the electrical properties and underlying crystal structure are discussed in the paper.

1. Introduction

Lead-based relaxor ferroelectric single crystals (RFSCs) have been intensely studied over recent decades due to their exceptional electromechanical coupling performance. Typical RFSCs include binary systems $Pb(Zn_{1/3}Nb_{2/3})O_3$-$PbTiO_3$ (PZN-PT) and $Pb(Mg_{1/3}Nb_{2/3})O_3$-$PbTiO_3$ (PMN-PT) [1, 2], as well as a ternary system, $Pb(In_{1/2}Nb_{1/2})O_3$-$Pb(Mg_{1/3}Nb_{2/3})O_3$-$PbTiO_3$ (PIN-PMN-PT), which possess enhanced properties in terms of high Curie temperature T_C and coercive field E_c. The origin of high piezoelectricity of RFSCs has long been an important issue. In this regard a widely accepted theory, proposed by Fu and Cohen [3], is the polarization rotation mechanism, the essence of which is that the polarization vectors can rotate freely within a lattice plane instead of being restricted to certain directions. This theory is supported by the observations of intermediate phases near the morphotropic phase boundary (MPB), for example, monoclinic M_A and M_C phases (space group *C*m and *P*m, resp.) [4]. On the other hand, the structure evolution of RFSCs under external fields of thermal, electrical, and/or mechanical stress is another important issue. From a viewpoint of application, as many piezoelectric devices are employed under a multi-field coupled environment, their electromechanical behavior usually deviates from a simple linear constitutive relationship, and as a result, those devices may suffer from failures that are unexpected based on individual factors. Therefore, it is of great importance to understand the structural evolution of RFSCs that governs their macroscopic properties using *in situ* techniques.

In this paper, we aim to study the electromechanical properties and crystal structure evolution with temperature for $Pb(In_{1/2}Nb_{1/2})O_3$-$Pb(Mg_{1/3}Nb_{2/3})O_3$-$PbTiO_3$ single crystals, via *in situ* single crystal neutron diffraction in conjunction with electrical characterization methods. The result leads to a good understanding of the phase transition behaviour in this material and associated RFSCs.

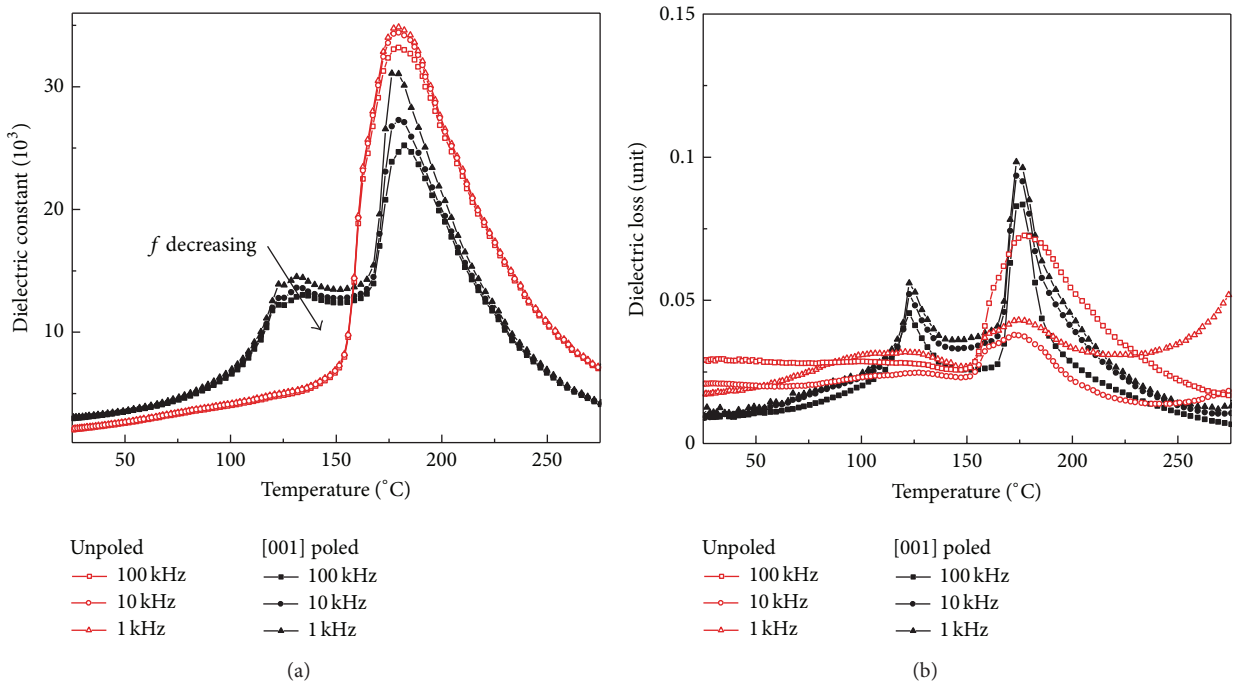

FIGURE 1: Temperature dependent dielectric constant (a) and loss (b) at several frequency points for the unpoled and [001]-poled 0.29PIN-0.44PMN-0.27PT single crystals.

2. Experiment

The near-MPB composition 0.29PIN-0.44PMN-0.27PT single crystals were grown using the vertical Bridgman technique [5]. Several [001]-oriented samples with dimension ~5 × 5 × 0.5 mm were cut from the near position in the crystal boule so as to minimize composition deviations (note that all pseudocubic crystallographic indexes are used throughout this paper). These crystals were silver-electroded on the 5 × 5 mm faces and two of them were poled along the [001] direction under an electric field of 10 kV/cm at room temperature. This poling method was found to sufficiently produce a high piezoelectric constant, d_{33}, of ~2000 pC/N, similar to the prevailing field-cooling method. In light of this, we neglected in the current study the issue of the dependence of the structure and electrical properties on poling electric fields. Temperature dependent dielectric spectra of both the states of crystals were measured in a furnace with a computer-interfaced *LCR* meter (*Agilent* 4284A) using 1 V_{rms} ac test signals. A ferroelectric analyzer system (TF2000, *AixCCCT*), including a bulk sample heating holder and a laser interferometer, was used to measure the electrical field-polarization (*P-E*) hysteresis loops and strain-field (*S-E*) curves on an unpoled sample. The *P-E* and *S-E* measurements were performed from room temperature to 200°C at every 5°C interval. *In situ* single crystal diffraction experiments were performed at ANSTO, using Wombat high intensity neutron diffractometer [6]. One of the poled crystals was fixed into a cryostat and then mounted at a four-circle Eulerian cradle which allowed quick crystal alignment. The sample was heated up to 200°C during the first run, and after cooling to 25°C now the depoled/unpoled crystals was again heated for the second run. The (002) reflections were mesh-scanned in the *H0L* scattering plane using a neutron wavelength of 1.838 Å.

3. Result and Discussion

Figures 1(a) and 1(b) show the dielectric constant and loss spectra, respectively, of 0.29PIN-0.44PMN-0.27PT single crystals as a function of temperature and frequency. As can be seen, both the [001]-poled and unpoled crystals exhibit a dielectric maximum temperature T_m ~ 182°C. Generally this peak position is attributed to the Curie temperature T_C where a transition from ferroelectric phases to paraelectric phases occurs, and it can well confirm the nominal composition for the crystals [2]. Aside from the same T_m, the poled and unpoled crystals display different characteristics; for example, the unpoled crystal only exhibits a broad T_m peak within the measured temperature range. It is therefore believed that the unpoled crystal is more typical of relaxor ferroelectric. This can be well understood since in RFSCs the relaxor nature of PMN (and PIN and others) competes with the normal ferroelectric order favoured by PT component.

By comparison, the poled crystal has an additional dielectric peak below T_m. Looking at it closely, two peaks may also be claimed from the permittivity spectra (Figure 1(a)), which are not found correspondingly from the loss spectra (Figure 1(b)). However, there is not a unanimous assignment of the associated phases in the literature. This is mainly due to the fact that the lattice parameters for the intermediate phases are quite close and even metrically the same. Another

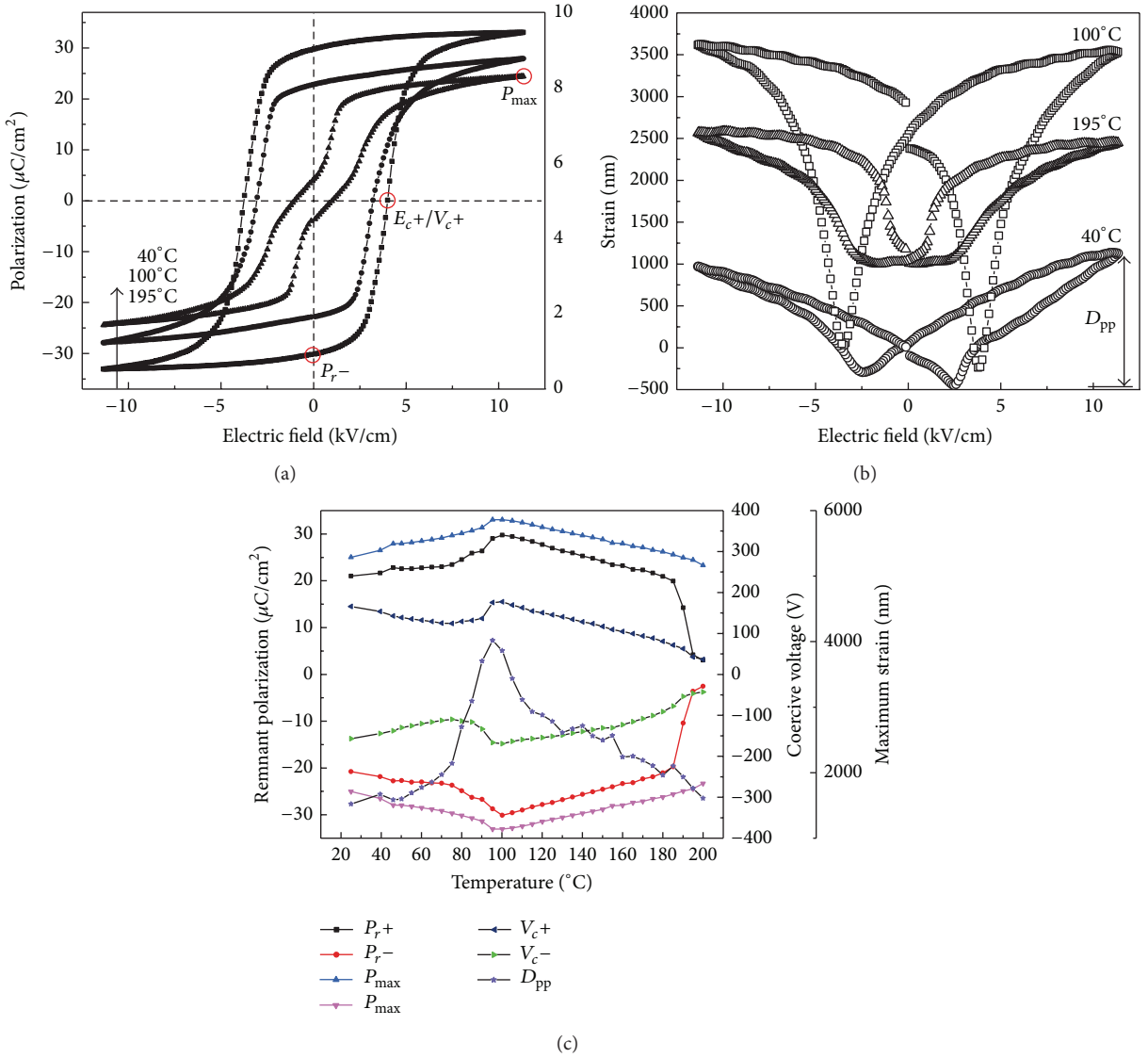

FIGURE 2: (a) *P-E* and (b) *S-E* hysteresis loops of 0.29PIN-0.44PMN-0.27PT single crystals, at three selected temperatures and (c) temperature dependence of the parameters deduced from those loops. Note that for clarity the *S-E* loops in (b) are vertically offset.

possible reason is that the stabilities of those phases are fragile and sensitive to many factors, for example, composition deviations [7]. In our case, it is believed that a transition sequence of *R* (rhombohedral)-M_A-M_C-*T* (tetragonal)-*C* is induced by heating, consistent with the polarization rotation pathway discussed by Noheda et al. [4]. The jump from M_A to M_C, which is different from the continuous *R*-M_A and M_C-*T* phase transitions, occurs in a wide temperature range 120–132°C. Besides, in this temperature range a frequency dependence of the dielectric permittivity can be observed (Figure 1(a)), which may therefore indicate diffuse characteristics for such a structural transition.

Figures 2(a) and 2(b) show the *P-E* hysteresis loops and *S-E* curves, respectively, at three selected temperatures, and the parameters drawn from those hysteresis loops versus temperature are plotted in Figure 2(c). An unpoled crystal was used for this series of measurements. At 40°C, a square *P-E* loop can be obtained with a saturated polarization P_s value of 28 μC/cm^2 and a coercive field E_c around 3.2 kV/cm. The corresponding *S-E* curve has a typical butterfly shape, and the maximum strain (defined as peak-to-peak displacement D_{pp}, see Figure 3(b)) can reach 1500 nm (0.3%). The strain curve shows a slight asymmetry as the positive half cycle is larger than the negative half, indicating that the domains are easier to switch to the positive *E* field direction. This could be due to the pinning effect of defects inside the crystal. With the temperature increases, the saturated/remnant polarization values gradually increase, and after reaching their maxima at ~100°C, they change into an opposite dependence and finally drop quickly near the T_m (Figure 2(c)). A similar trend can be found for the maximum strain, and the field-induced strain is significantly enhanced near 100°C. The strain curve

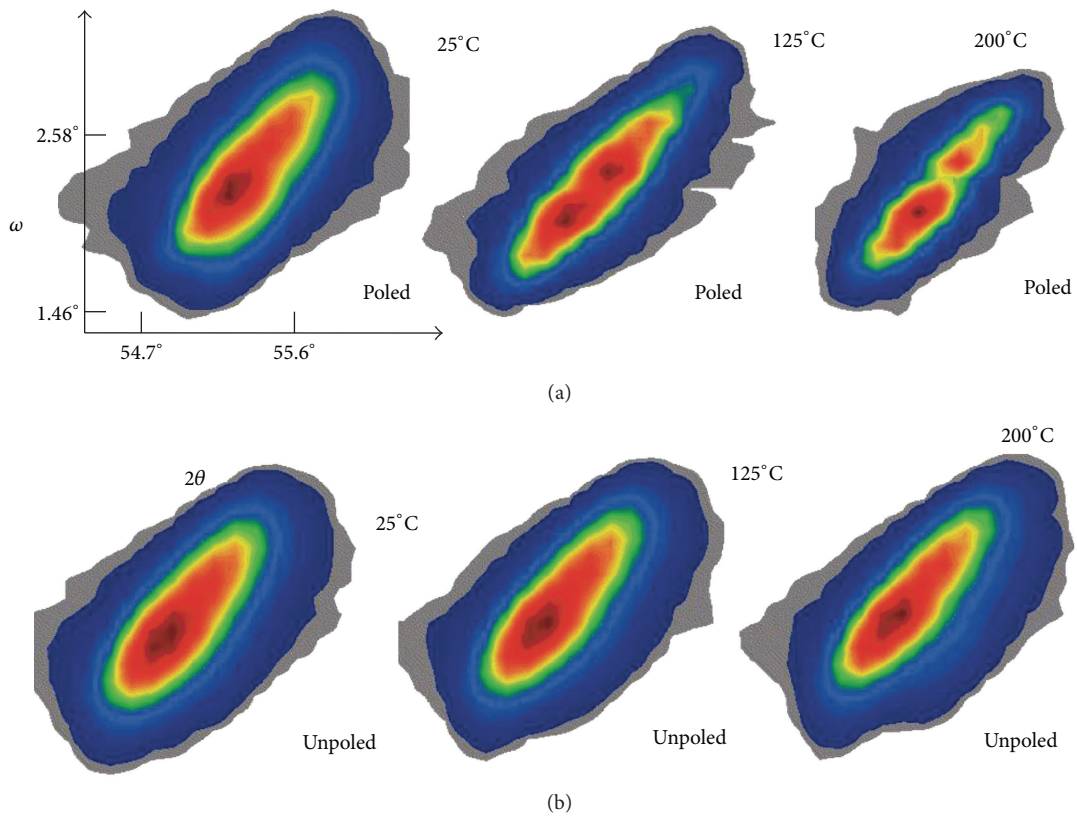

Figure 3: Contour of (002) reflection for [001]-poled (upper row) and unpoled (lower row) 0.29PIN-0.44PMN-0.27PT single crystals, at three selected temperatures.

at 100°C (Figure 2(b)) reveals that a great portion of strain is achieved during the course of domain switching, suggesting that domain switching is highly facilitated by the M_A-M_C transition where the polarization vector jumps from the (110) plane to (100) plane. However, it is also very likely that such a transition itself can make an important contribution to the total strain due to a discontinuous change in lattice dimensions. In contrast, the variation of coercive field shows a different behavior; basically it always decreases with temperature except for a jump occurring near 100°C. It is evident that all those parameters reflect a phase transition point at 100°C, near the M_A-M_C transition temperature range, in good agreement with the dielectric spectroscopic results. The difference in the transition temperature obtained from these two techniques may be because the electrical field strength levels are remarkably different.

Another interesting phenomenon observed is that near T_m, the spontaneous polarization does not disappear instantly. Instead an antiferroelectric behavior can be induced at this critical temperature. As shown in Figure 2(a), the *P-E* hysteresis loop at 195°C develops into a double loop shape. The remnant polarization value is not zero, suggesting the coexistence of ferroelectric order to a certain extent. Besides, the strain curve obtained here is more typical of an antiferroelectric as no negative strain can be induced by electric field; that is, the crystal cannot contract relative to a zero-field state. Zhao et al. [8] reported a similar phenomenon in 0.76PMN-0.24PT single crystals near the M_A-M_C temperature (which they called T_d, depolarization temperature). They explained that a macrodomain state to microdomain state transition occurs when heating the poled crystal across T_d and that this transition is responsible for their observed "triple-like" loops. Compared to this report, our result is different since in our case the double *P-E* loops are observed only near T_m.

Figure 3 shows the evolution of the contours of (002) reflection resulting from *in situ* neutron diffraction measurements. Generally, single diffraction examines only one Bragg peak at each reflection position, irrespective of the symmetry of a crystal. For ferroelectric materials, however, due to the presence of ferroelectric domains which act as a certain type of structure twinning, multiple twined Bragg peaks can possibly be present for one reflection [9, 10]. In this case, at 25°C, the (002) reflection contours appear to have a single component for both the unpoled and poled states. This agrees with the rhombohedral symmetry of the crystals as known from the previous discussion on electrical measurements. When the crystals are heated up to 200°C, the (002) reflection for the unpoled state changes only a little in position as a result of thermal expansions, while basically remains a single component profile. Note that the small overall shift of the reflections and the underlying lattice changes are not addressed here. By contrast, for the poled crystal two components with similar magnitude can be observed on the (002)

reflection measured at 125°C. The two components have different 2θ diffraction angles as well as different ω rocking angle, implying that the three lattice vectors herein are no longer equivalent as in an R symmetry. We believe that such a splitting is a clear evidence for the tetragonal symmetry that the poled crystal possesses around this critical temperature. The aforementioned monoclinic symmetries, however, also possibly give rise to such a diffraction result; that is, it is not sufficient to assign a T symmetry from this (002) reflection alone. Moreover, the (002) reflection for the poled crystal measured at 200°C, a temperature well above T_m, shows a weak peak component together with a main component, implying that the crystal has not totally been of a cubic phase at the current temperature. A very possible scenario is that there are some polar domains/regions coexisting with the major nonpolar paraelectric phase in the crystal, and this may provide a structural basis for the apparent antiferroelectric behavior shown in the *P-E* and *S-E* hysteresis loops. On the other hand, it is difficult to ascertain an actual length scale for the residual polar domains based upon the current diffraction results. Real space ferroelectric domain imaging techniques, for example, piezoresponse force microscopy, might be employed to probe this information at the nanoscale [11].

4. Summary

The dielectric property, ferroelectric polarization, and strain hysteresis loop as well as crystal structure for relaxor ferroelectric 0.29PIN-0.44PMN-0.27PT single crystals are characterized over a temperature region from about room temperature to 200°C. A combinational analysis of those characterization results has revealed the phase transition behavior within this temperature region, and very good agreement can be found between the structure of the crystals and their macroscopic electrical properties.

Acknowledgments

Qian Li, Yun Liu, and Ray Withers acknowledge financial support from the Australian Research Council (ARC) in the form of an ARC Discovery Grant. Yun Liu also acknowledges support from the ARC Future Fellowships program. The authors also thank the Australian Institute of Nuclear Science and Engineering (ANSIE) for financial support to access the national neutron facilities at ANSTO.

References

[1] S.-E. Park and T. R. Shrout, "Ultrahigh strain and piezoelectric behavior in relaxor based ferroelectric single crystals," *Journal of Applied Physics*, vol. 82, no. 4, pp. 1804–1811, 1997.

[2] X. Li and H. Luo, "The growth and properties of relaxor-based ferroelectric single crystals," *Journal of the American Ceramic Society*, vol. 93, no. 10, pp. 2915–2928, 2010.

[3] H. Fu and R. E. Cohen, "Polarization rotation mechanism for ultrahigh electromechanical response in single-crystal piezoelectrics," *Nature*, vol. 403, no. 6767, pp. 281–283, 2000.

[4] B. Noheda, D. E. Cox, G. Shirane, S.-E. Park, L. E. Cross, and Z. Zhong, "Polarization rotation via a monoclinic phase in the piezoelectric 92% $PbZn_{1/3}Nb_{2/3}O_3$-8%$PbTiO_3$," *Physical Review Letters*, vol. 86, no. 17, pp. 3891–3894, 2001.

[5] X. Wang, Z. Xu, Z. Li, F. Li, H. Chen, and S. Fan, "Growth of the relaxor based ferroelectric single crystals $Pb(In_{1/2}Nb_{1/2})O_3$-$Pb(Mg_{1/3}Nb_{2/3})O_3$-$PbTiO_3$ by vertical Bridgman technique," *Ferroelectrics*, vol. 401, no. 1, pp. 173–180, 2010.

[6] A. J. Studer, M. E. Hagen, and T. J. Noakes, "Wombat: the high-intensity powder diffractometer at the OPAL reactor," *Physica B*, vol. 385, pp. 1013–1015, 2006.

[7] Z. Li, Z. Xu, X. Yao, and Z.-Y. Cheng, "Phase transition and phase stability in [110]-, [001]-, and [111]-oriented $0.68Pb(Mg_{1/3}Nb_{2/3})O_3$-$0.32PbTiO_3$ single crystal under electric field," *Journal of Applied Physics*, vol. 104, no. 2, Article ID 024112, 2008.

[8] X. Zhao, J. Wang, Z. Peng, H. L. W. Chan, C. L. Choy, and H. Luo, "Triple-like hysteresis loop and microdomain-macrodomain transformation in the relaxor-based $0.76Pb(Mg_{1/3}Nb_{2/3})O_3$-$0.24PbTiO_3$ single crystal," *Materials Research Bulletin*, vol. 39, no. 2, pp. 223–230, 2004.

[9] Q. Li, Y. Liu, J. Wang et al., "Structural transitions in [001]/[111]-oriented $0.26Pb(In_{1/2}Nb_{1/2})O_3$-$0.46Pb(Mg_{1/3}Nb_{2/3})O_3$-$0.28PbTiO_3$ single crystals probed via neutron diffraction and electrical characterization," *Jornal of Applied Physics*, vol. 113, Article ID 154104, 2013.

[10] Z.-G. Ye, B. Noheda, M. Dong, D. Cox, and G. Shirane, "Monoclinic phase in the relaxor-based piezoelectric/ferroelectric $Pb(Mg_{1/3}Nb_{2/3})O_3$-$PbTiO_3$ system," *Physical Review B*, vol. 64, no. 18, Article ID 184114, 2001.

[11] Q. Li, Y. Liu, R. L. Withers, Y. Wan, Z. Li, and Z. Xu, "Piezoresponse force microscopy studies on the domain structures and local switching behavior of $Pb(In_{1/2}Nb_{1/2})O_3$-$Pb(Mg_{1/3}Nb_{2/3})O_3$-$PbTiO_3$ single crystals," *Journal of Applied Physics*, vol. 112, Article ID 052006, 2012.